

Oscillator Strengths in ONIOM Excited State Calculations

Marco Caricato,^{*,†} Thom Vreven,[‡] Gary W. Trucks,[†] and Michael J. Frisch[†]

*Gaussian, Inc., 340 Quinipiac St., Bldg. 40, Wallingford, Connecticut 06492, United States,
and Program in Bioinformatics and Integrative Biology, University of Massachusetts
Medical School, Worcester, Massachusetts 01605, United States*

Received November 2, 2010

Abstract: We compute oscillator strengths with the ONIOM (Our own N-layer Integrated molecular Orbital molecular Mechanics) hybrid method between ground and valence excited states and compare the results with the high level of theory equation of motion coupled cluster singles and doubles (EOM-CCSD). This work follows our previous studies in which we validated the ability of ONIOM to compute accurate transition energies compared to EOM-CCSD. We test various levels of theory and molecular systems, as well as the effect of the link atom bond length. Our results show that oscillator strengths can be accurately computed with ONIOM, provided that a sensible choice of the partitioning and of the low level method is made. Being able to calculate both the transition energy and the oscillator strength, ONIOM represents a promising approach to completely characterize valence excited states of molecules that are too large to be studied with a conventional high-accuracy method.

1. Introduction

Methods that combine two (or more) levels of theory are now widely used to study ground state phenomena and processes of large systems.¹ Such “hybrid methods” divide the system into a region of major interest treated at a high level of theory, while the rest (substituent effect) is treated at a lower and less computationally demanding level. Most of these methods combine a quantum mechanical level with a molecular mechanical level, QM/MM,^{1–4} and the energy is expressed as a summation. On the other hand, the ONIOM (Our own N-layer Integrated molecular Orbital molecular Mechanics)^{5–15} energy is formulated as extrapolation. Therefore, it can easily combine more than two computational levels as well as integrate two or more different quantum mechanical levels, QM/QM. In ONIOM, open valencies in the *model* system generated from cutting covalent bonding between regions are saturated with link atoms (typically hydrogens). A link atom is placed in the same direction of the atom it replaces, with a distance scaled by a factor

proportional to the ratio between the original bond length and the typical bond distance of the atoms involved.

While the use of hybrid methods for ground state problems has been well documented, their use in excited state calculation is still limited. This is especially so when two QM levels of theory are combined.¹ In two recent studies,^{16,17} we investigated the ability of the ONIOM hybrid method to reproduce equation of motion coupled cluster singles and doubles (EOM-CCSD)^{18–24} vertical excitation energies. The EOM-CCSD results on the entire system (the *target*) were used as a reference, and the performance of ONIOM was compared either to conventional calculations with a lower level of theory on the entire system or to EOM-CCSD only on the core region. We analyzed the effect of the partitioning, of the choice of the low level methods and basis sets, and of the link atom bond length. We found that, provided certain guidelines for the partitioning^{15,17} are followed, ONIOM is able to accurately approximate EOM-CCSD while providing a drastic reduction in computational time. ONIOM with time-dependent density functional theory (TDDFT) as the low level provided the best overall performance. Also, the exact value of the link atom bond length did not significantly influence the ONIOM results, analogous to what was found for ground state calculations;²⁵ hence, the same definition for the link atom bond length used for the ground state can

* To whom correspondence should be addressed. E-mail: marco@gaussian.com.

[†] Gaussian, Inc.

[‡] University of Massachusetts.

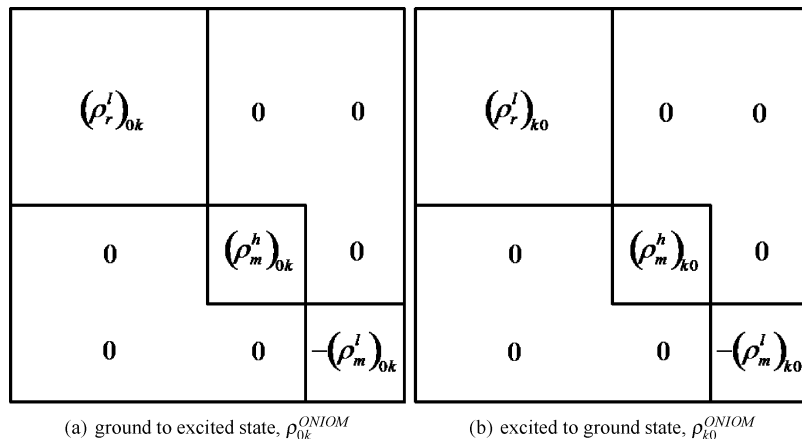


Figure 1. Integrated ONIOM transition densities.

be retained for excited state calculations. Finally, we also proposed several new guidelines for using ONIOM in excited states studies.¹⁷

Although the energy is the primary quantity that needs to be considered to assess the performance of ONIOM, transition properties are also important for the investigation of electronic excitations. In this paper, we focus on the oscillator strength since this quantity is directly related to the intensity of a transition. Our comparison will be with this property computed for the entire system at the *high* level of theory, because this is the reference value that we aim to reproduce (*target*). We consider two molecular systems from our previous works and two new systems with large oscillator strengths. For this paper, as in our previous studies, we limit our investigation to valence states. The *model* system for each molecule is chosen according to the ONIOM guidelines for partitioning¹⁵ and based on the results of our previous studies.^{16,17} For this *model* system, the ONIOM *high* level calculation is performed at the *target* level of theory while various levels of theory are tested for the ONIOM *low* level calculations. Only QM/QM combinations are considered in this work, as in refs 16 and 17, since a MM method in the *low* level does not directly contribute to the excited state calculation.

The results in this paper show that transition properties can be accurately computed with ONIOM, and that the same considerations employed when computing the transition energy apply to the oscillator strength.

The paper is organized as follows. The formulas for the calculation of ONIOM transition energies and properties are reported in section 2. Computational details are given in section 3. The results of the calculations are presented in section 4, while section 5 contains a discussion of these results and concluding remarks.

2. Theory

The ONIOM energy for a two-layer system with mechanical embedding is written as an extrapolation:

$$E^{ONIOM} = E_{model}^{high} + E_{real}^{low} - E_{model}^{low} \quad (1)$$

where *real* and *model* refer to the full system and to the core region, respectively. The transition energy (ΔE) in the

ONIOM scheme can be expressed as the difference of the ONIOM energies of the *k*th and the ground states:

$$\begin{aligned} \Delta E^{ONIOM} &= E^{k,ONIOM} - E^{ONIOM} \\ &= (E_{model}^{k,high} + E_{real}^{k,low} - E_{model}^{k,low}) - (E_{model}^{high} + E_{real}^{low} - E_{model}^{low}) \\ &= (E_{model}^{k,high} - E_{model}^{high}) + (E_{real}^{k,low} - E_{real}^{low}) - (E_{model}^{k,low} - E_{model}^{low}) \\ &= \Delta E_{model}^{high} + \Delta E_{real}^{low} - \Delta E_{model}^{low} \end{aligned} \quad (2)$$

The ONIOM oscillator strength, f^{ONIOM} , is calculated as

$$f^{ONIOM} = \frac{2}{3} \Delta E^{ONIOM} D^{ONIOM} \quad (3)$$

where D^{ONIOM} is the ONIOM dipole strength defined as

$$D^{ONIOM} = \sum_i (\mu_i^{ONIOM})_{0k} \times (\mu_i^{ONIOM})_{k0} \quad i = x, y, z \quad (4)$$

and $(\mu_i^{ONIOM})_{0k}$ are the components of the integrated ONIOM transition dipole:

$$(\mu_i^{ONIOM})_{0k} = Tr[(\rho_m^h)_{0k}(\mu_m^h)_i] + Tr[(\rho_r^l)_{0k}(\mu_r^l)_i] - Tr[(\rho_m^l)_{0k}(\mu_m^l)_i] \quad (5)$$

where $\mu_{m/r}^{h/l}$ are the dipole integrals of the various subcalculations (h/l indicates the *high* or *low* level of theory, and m/r indicates the *model* or *real* system). A similar expression is used to compute $(\mu_i^{ONIOM})_{k0}$. In order to compute transition properties, integrated ONIOM transition densities must be defined, ρ_{0k}^{ONIOM} and ρ_{k0}^{ONIOM} . These are shown in Figure 1, where the ground to excited state (ρ_{0k}^{ONIOM}) and the excited to ground state (ρ_{k0}^{ONIOM}) densities are represented in terms of the transition densities of the subcalculations. Two different integrated transition density matrices are necessary when a method like EOM-CCSD is used since this method has a non-Hermitian Hamiltonian.²⁰ However, $\rho_{0k} = \rho_{k0}$ for methods like configuration interaction singles (CIS), time-dependent Hartree–Fock (TDHF), and TDDFT.

Alternatively, a simpler formula may be used to compute f^{ONIOM} by directly integrating the oscillator strengths of the subcalculations:

$$\tilde{f}^{ONIOM} = \tilde{f}_{model}^{high} + \tilde{f}_{real}^{low} - \tilde{f}_{model}^{low} \quad (6)$$

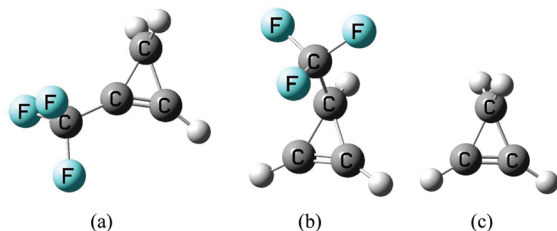


Figure 2. Structures of 1-trifluoro-methyl-cyclopropene (a), 3-trifluoro-methyl-cyclopropene (b), and the *model* system (c).

which does not require the integration of the transition dipole. \tilde{f}^{ONIAM} is an approximation of f^{ONIAM} in eq 3, as it is easy to verify that $f^{\text{ONIAM}} = \tilde{f}^{\text{ONIAM}} + \text{cross terms}$. However, since the subcalculation transition dipoles are needed for both f^{ONIAM} and \tilde{f}^{ONIAM} , there is not a particular computational advantage in using the latter. Therefore, we will not further consider \tilde{f}^{ONIAM} .

3. Computational Details

The ground state geometries of the entire molecules are optimized at the B3LYP level with the 6-311+G** basis set and subsequently used for all the excited state calculations. The *target* oscillator strength and transition energy (i.e., that we want to reproduce with ONIAM), f^{target} and ΔE^{target} , respectively, are computed at the EOM-CCSD/6-311+G** level of theory on the entire (*real*) system. For ONIAM, only one level of theory is used in the *high* level calculation on the *model* system: EOM-CCSD/6-311+G** (i.e., the same as the *target*). For the *low* level calculations (on the *model* and *real* systems), we test CIS, TDHF, and TDDFT (with the B3LYP functional^{26–28}) with the 6-311+G** basis set. We also consider EOM-CCSD/6-31+G* as a *low* level method. In the following, we refer to the 6-311+G** and 6-31+G* basis sets as “L” and “M”, respectively, for consistency with refs 16 and 17. For the ketene, we also test three functionals other than B3LYP, namely, CAM-B3LYP,^{29,30} BLYP,^{31,32} and LC-BLYP.^{31–34} All of the calculations are performed with the Gaussian 09 suite of programs.³⁵ In summary, we consider the following ONIAM combinations:

- ONIAM(EOM/L:EOM/M)
- ONIAM(EOM/L:TDDFT/L)
- ONIAM(EOM/L:TDHF/L)
- ONIAM(EOM/L:CIS/L)

In the next section, these ONIAM combinations are compared with the conventional calculations at the corresponding *low* level of theory on the entire system ($f_{\text{real}}^{\text{low}}$ and $\Delta E_{\text{real}}^{\text{low}}$), and with the *high* level of theory on the *model* system ($f_{\text{model}}^{\text{high}}$ and $\Delta E_{\text{model}}^{\text{high}}$). In fact, $f_{\text{real}}^{\text{low}}$ and $f_{\text{model}}^{\text{high}}$ can be considered as approximations of f^{target} when the latter is computationally too expensive to evaluate (equivalently $\Delta E_{\text{real}}^{\text{low}}$ and $\Delta E_{\text{model}}^{\text{high}}$ for ΔE^{target}). Therefore, it is interesting to test ONIAM versus these approximated conventional calculations.

4. Results

The ability of ONIAM to reproduce the *target* oscillator strengths is tested on four molecular systems, shown in Figures 2–4 with their respective *model* systems. Although

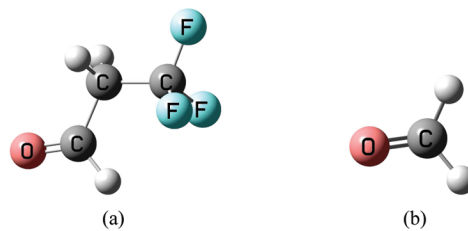


Figure 3. Structures of 3,3,3-trifluoropropanal (a) and the *model* system (b).

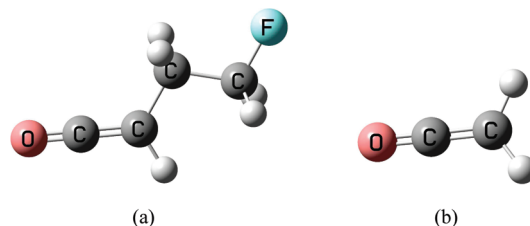


Figure 4. Structures of 4-fluorobut-1-en-1-one (a) and the *model* system (b).

the number of test cases in this work is limited, they are analyzed in great detail, and a large variety of possible sources of errors is considered. Therefore, even though the results presented in this section are preliminary, they provide useful insight on the ONIAM accuracy for this property. The first two systems, the substituted cyclopropenes, appeared in our previous works where we analyzed the dependence of ΔE^{ONIAM} on the choice of the *model* system, the *low* level of theory, and the link atom bond length.^{16,17} These systems represent good candidates to study the ONIAM performance on transition properties because we already know how the various choices of the subcalculations influence the transition energy. For this reason, we only consider the *model* systems that performed best in refs 16 and 17, which indeed follow the ONIAM guidelines for the partitioning.¹⁵ We consider the second transition for both systems since it has a larger oscillator strength. Unfortunately, we could not select other systems from our previous studies because f^{target} was negligible and thus not suitable for this investigation. The two new systems chosen for this study are 3,3,3-trifluoropropanal and 4-fluorobut-1-en-1-one (in the following, we will refer to these systems as the “aldehyde” and the “ketene”, respectively), for which we examine two bright states. Both molecules are forced in the C_s geometry. All of the transitions considered are $\pi \rightarrow \pi^*$. In addition to the oscillator strength, we also discuss the ONIAM performance on ΔE in order to understand how their relative performances are related.

For the cyclopropenes, the transition energies are reported in Table 1 and the oscillator strengths in Table 2. An interesting aspect of these two molecules is that the same *model* system can be used for both (albeit with some geometrical differences due to the different *real* systems’ geometries). As discussed in ref 16, ΔE^{ONIAM} is a very good estimates of ΔE^{target} for both molecules, especially with EOM/M and TDDFT/L in the *low* level. Although $\Delta E_{\text{model}}^{\text{high}}$ for the first system is very close to the *target*, ONIAM(EOM/L:EOM/M) is even closer, while the error with ONIAM-(EOM/L:TDDFT/L) is below 0.1 eV. For the second system,

Table 1. Transition Energies (eV) for the Substituted Cyclopropenes

X	1-trifluoro-methyl-cyclopropene			3-trifluoro-methyl-cyclopropene		
	ΔE_{real}^a	$\Delta E_{\text{model}}^b$	$\Delta E_{\text{ONIOM},c}^c$	ΔE_{real}^a	$\Delta E_{\text{model}}^b$	$\Delta E_{\text{ONIOM},c}^c$
EOM/L	7.09 ^d	7.10 ^e		7.48 ^d	7.04 ^e	
EOM/M	7.15	7.15	7.09	7.57	7.10	7.52
TDDFT/L	6.19	6.27	7.02	6.63	6.20	7.48
TDHF/L	6.67	6.58	7.18	6.98	6.57	7.46
CIS/L	6.99	6.86	7.22	7.29	6.85	7.49

^a Conventional calculation on the *real* system. ^b Conventional calculation on the *model* system. ^c ONIOM(EOM/L:X), where X is the level of theory specified in the first column. ^d $\Delta E_{\text{target}}^{\text{target}}$: EOM/L level on the *real* system. ^e $\Delta E_{\text{model}}^{\text{high}}$: EOM/L level on the *model* system.

Table 2. Oscillator Strengths for the Substituted Cyclopropenes

X	1-trifluoro-methyl-cyclopropene			3-trifluoro-methyl-cyclopropene		
	f_{real}^a	f_{model}^b	$f_{\text{ONIOM},c}^c$	f_{real}^a	f_{model}^b	$f_{\text{ONIOM},c}^c$
EOM/L	0.1128 ^d	0.0792 ^e		0.0810 ^d	0.0783 ^e	
EOM/M	0.1124	0.0794	0.1120	0.0800	0.0784	0.0799
TDDFT/L	0.1020	0.0702	0.1155	0.0671	0.0677	0.0770
TDHF/L	0.1474	0.1202	0.1022	0.1209	0.1205	0.0772
CIS/L	0.1748	0.1493	0.0977	0.1537	0.1500	0.0789

^a Conventional calculation on the *real* system. ^b Conventional calculation on the *model* system. ^c ONIOM(EOM/L:X), where X is the level of theory specified in the first column. ^d $f_{\text{target}}^{\text{target}}$: EOM/L level on the *real* system. ^e $f_{\text{model}}^{\text{high}}$: EOM/L level on the *model* system.

Table 3. Transition Energies (eV) and Oscillator Strengths for the Aldehyde

X	ΔE_{real}^a	$\Delta E_{\text{model}}^b$	$\Delta E_{\text{ONIOM},c}^c$	f_{real}^a	f_{model}^b	$f_{\text{ONIOM},c}^c$
EOM/L	9.36 ^d	10.00 ^e		0.1423 ^f	0.1577 ^g	
EOM/M	9.41	10.13	9.28	0.1369	0.1854	0.1161
TDDFT/L	8.60	9.50	9.10	0.1171	0.1277	0.1416
TDHF/L	9.28	9.38	9.90	0.2391	0.2422	0.1582
CIS/L	9.66	9.74	9.92	0.2628	0.2824	0.1439

^a Conventional calculation on the *real* system. ^b Conventional calculation on the *model* system. ^c ONIOM(EOM/L:X), where X is the level of theory specified in the first column. ^d $\Delta E_{\text{target}}^{\text{target}}$: EOM/L level on the *real* system. ^e $\Delta E_{\text{model}}^{\text{high}}$: EOM/L level on the *model* system. ^f $f_{\text{target}}^{\text{target}}$: EOM/L level on the *real* system. ^g $f_{\text{model}}^{\text{high}}$: EOM/L level on the *model* system.

ONIOM provides a large improvement over $\Delta E_{\text{model}}^{\text{high}}$ and $\Delta E_{\text{real}}^{\text{low}}$ for all of the *low* level methods. Table 2 shows that the same good performance is shared by the oscillator strength calculations. In this case, the first molecule shows the larger improvement by using ONIOM instead of the conventional calculations ($f_{\text{model}}^{\text{high}}$ and $f_{\text{real}}^{\text{low}}$) to approximate the *target*, except for EOM/M where $f_{\text{real}}^{\text{low}}$ is very close to $f_{\text{target}}^{\text{target}}$; nevertheless, the ONIOM results are very close to the *target* even for EOM/M. For the second molecule, $f_{\text{model}}^{\text{high}}$ is already very close to $f_{\text{target}}^{\text{target}}$, but the ONIOM results also have very small errors. Additionally, ONIOM always improves over $f_{\text{real}}^{\text{low}}$.

The results for the aldehyde are reported in Table 3. The performances of ONIOM(EOM/L:EOM/M) and ONIOM(EOM/L:TDDFT/L) on the transition energy are very good. The former maintains an already small $\Delta E_{\text{real}}^{\text{low}}$ error, and the latter improves on both $\Delta E_{\text{model}}^{\text{high}}$ and $\Delta E_{\text{real}}^{\text{low}}$. This is not the case with CIS/L and TDHF/L in the *low* level. For these two methods, the improvement over $\Delta E_{\text{model}}^{\text{high}}$ is in the right direction, but it is not enough to provide a good estimate of $\Delta E_{\text{target}}^{\text{target}}$. The reason is probably the lack of correlation effects, which are important for obtaining a reliable description of the substituent effect. $f_{\text{target}}^{\text{target}}$ is well reproduced with ONIOM and TDDFT/L, TDHF/L, and CIS/L as *low* methods. The poor performance of ONIOM(EOM/L:EOM/M) for the

Table 4. Basis Set Dependence of the Transition Energies (eV) and Oscillator Strengths for the Aldehyde

X	ΔE_{real}^a	$\Delta E_{\text{model}}^b$	$\Delta E_{\text{ONIOM},c}^c$	f_{real}^a	f_{model}^b	$f_{\text{ONIOM},c}^c$
EOM/L	9.36 ^d	10.00 ^e		0.1423 ^f	0.1577 ^g	
EOM/M	9.41	10.13	9.28	0.1369	0.1854	0.1161
CIS/L	9.66	9.74	9.92	0.2628	0.2824	0.1439
CIS/M	9.71	9.84	9.87	0.2623	0.3097	0.1253

^a Conventional calculation on the *real* system. ^b Conventional calculation on the *model* system. ^c ONIOM(EOM/L:X), where X is the level of theory specified in the first column. ^d $\Delta E_{\text{target}}^{\text{target}}$: EOM/L level on the *real* system. ^e $\Delta E_{\text{model}}^{\text{high}}$: EOM/L level on the *model* system. ^f $f_{\text{target}}^{\text{target}}$: EOM/L level on the *real* system. ^g $f_{\text{model}}^{\text{high}}$: EOM/L level on the *model* system.

Table 5. Transition Energies (eV) and Oscillator Strengths for the Ketene

X	ΔE_{real}^a	$\Delta E_{\text{model}}^b$	$\Delta E_{\text{ONIOM},c}^c$	f_{real}^a	f_{model}^b	$f_{\text{ONIOM},c}^c$
EOM/L	10.09 ^d	10.74 ^e		0.7675 ^f	0.9801 ^g	
EOM/M	10.16	10.82	10.07	0.6392	0.9825	0.6355
TDDFT/L	9.31	10.37	9.67	0.3473	0.8211	0.4385
TDHF/L	10.50	10.81	10.42	0.8353	0.7804	1.0336
CIS/L	10.87	11.18	10.42	0.5967	0.9768	0.6034

^a Conventional calculation on the *real* system. ^b Conventional calculation on the *model* system. ^c ONIOM(EOM/L:X), where X is the level of theory specified in the first column. ^d $\Delta E_{\text{target}}^{\text{target}}$: EOM/L level on the *real* system. ^e $\Delta E_{\text{model}}^{\text{high}}$: EOM/L level on the *model* system. ^f $f_{\text{target}}^{\text{target}}$: EOM/L level on the *real* system. ^g $f_{\text{model}}^{\text{high}}$: EOM/L level on the *model* system.

oscillator strength can be explained by the inadequacy of the “M” basis set for the *model* system calculation. Indeed, repeating the calculation at the CIS level with this basis set (reported in Table 4), we find that the trends EOM/L → EOM/M and CIS/L → CIS/M are similar. Although $f_{\text{ONIOM}}^{\text{target}}$ with EOM/M in the *low* level is not unreasonable, it certainly increases the error compared to $f_{\text{model}}^{\text{high}}$ and $f_{\text{real}}^{\text{low}}$.

The last system is a ketene for which we consider a very bright transition, $f_{\text{target}}^{\text{target}} = 0.7675$. The results are reported in Table 5. ONIOM improves the agreement with $\Delta E_{\text{target}}^{\text{target}}$ with all the *low* level methods compared to $\Delta E_{\text{model}}^{\text{high}}$ and $\Delta E_{\text{real}}^{\text{low}}$ (for EOM/M, the improvement is small, as $\Delta E_{\text{real}}^{\text{low}}$ is already

Table 6. Functional Dependence of the Transition Energies (eV) and Oscillator Strengths for the Ketene

X	ΔE_{real}^a	$\Delta E_{\text{model}}^b$	$\Delta E_{\text{ONIOM},c}$	f_{real}^a	f_{model}^b	$f_{\text{ONIOM},c}$
EOM/L	10.09 ^d	10.74 ^e		0.7675 ^f	0.9801 ^g	
B3LYP/L	9.31	10.37	9.67	0.3473	0.8211	0.4385
CAM-B3LYP/L	9.75	10.49	9.99	0.6355	0.8399	0.7448
BLYP/L	9.80	10.09	10.45	0.1634	0.7500	0.2581
LC-BLYP/L	10.18	10.67	10.25	0.8521	0.8784	0.9480

^a Conventional calculation on the *real* system. ^b Conventional calculation on the *model* system. ^c ONIOM(EOM/L:X), where X is the level of theory specified in the first column. ^d ΔE_{target} : EOM/L level on the *real* system. ^e $\Delta E_{\text{model}}^{\text{high}}$: EOM/L level on the *model* system. ^f f_{target} : EOM/L level on the *real* system. ^g $f_{\text{model}}^{\text{high}}$: EOM/L level on the *model* system.

Table 7. Transition Energies (eV) and Oscillator Strengths for the Ketene with the daug-cc-pVTZ Basis Set

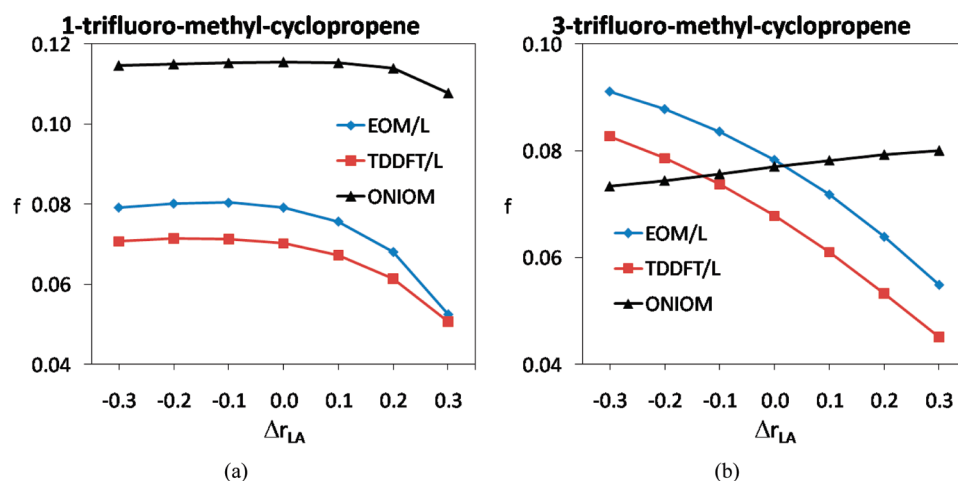
	ΔE_{real}^a	$\Delta E_{\text{model}}^b$	f_{real}^a	f_{model}^b
EOM		10.48		0.7088
B3LYP	9.17	10.25	0.3246	0.4940
TDHF	10.35	10.64	0.5330	0.5803
CIS	10.69	10.91	0.6253	0.6669
CAM-B3LYP	9.55	10.18	0.3101	0.5930
BLYP	9.67	10.75	0.1607	0.4010
LC-BLYP	10.07	10.52	0.6095	0.7261

^a Conventional calculation on the *real* system. ^b Conventional calculation on the *model* system.

very close to ΔE_{target}). For the oscillator strength, the ONIOM performance varies depending on the *low* level method. f_{ONIOM} with EOM/M is very close to f_{target} . ONIOM(EOM/L:TDDFT/L) and ONIOM(EOM/L:CIS/L) move $f_{\text{model}}^{\text{high}}$ and $f_{\text{real}}^{\text{low}}$ in the right direction; although for TDDFT/L, $f_{\text{model}}^{\text{high}}$ is closer to the *target* than f_{ONIOM} . ONIOM(EOM/L:TDHF/L) is very close to $f_{\text{model}}^{\text{high}}$, but the correction goes in the wrong direction. The poor performance of TDDFT/L as a *low* level in this case, contrary to the previous ones, is related to the choice of the particular functional: B3LYP does not satisfactorily reproduce the long-range effect of the substituent group. This can be recovered by employing a functional that better describes this effect, such as CAM-B3LYP. ONIOM(EOM/L:CAM-B3LYP/L) provides results in very good agreement with the *target* calculation, both for the energy and the oscillator strength, see Table 6. The lack of a correct description of the long-range effect in B3LYP as a cause of its poor performance is confirmed by considering the results obtained with the BLYP functional with and without long-range corrections, also in

Table 6. Although BLYP is not a good choice for computing excited state energy and properties with ONIOM and in conventional calculations,³⁶ the trend between B3LYP and BLYP when long-range corrections are introduced is similar. This problem could be partly overcome by considering a much larger basis set, and in Table 7 we report the data computed with the daug-cc-pVTZ basis, which has a double set of diffuse functions. This basis set is too large for performing the calculation on the entire system at the EOM-CCSD level, but the results in Table 7 show that the difference between B3LYP and CAM-B3LYP (and BLYP and LC-BLYP) is greatly reduced.

Finally, we examine the effect of the link atom bond length (r_{LA}) on the oscillator strength by computing it when moving away from the standard r_{LA} value (r_{LA}^0) in a range of ± 0.3 Å. We only consider one *low* level method for the sake of clarity (we choose TDDFT since it provides on average the best performance). Figure 5 reports the variation of f_{ONIOM} as well as $f_{\text{model}}^{\text{high}}$ and $f_{\text{real}}^{\text{low}}$ as a function of the r_{LA} shift for the substituted cyclopropenes: $r_{\text{LA}}^0 = 1.067$ Å and $= 1.092$ Å, respectively. The figures show that ONIOM only has a small dependence on r_{LA} for the oscillator strength. In Figure 5a, the variation is also small for the subcalculations (in the range of ± 0.1 Å), whereas in Figure 5b, the *model* system calculations have the same dependence on r_{LA} . Thus, f_{ONIOM} benefits from the error cancellation. These results are similar to the behavior of ΔE_{ONIOM} for the same systems (compare with Figures 19 and 20 in ref 17). For the aldehyde, we consider the shift of the transition energy ($\Delta E_{\text{model}}^{\text{high}}$, $\Delta E_{\text{model}}^{\text{low}}$ and ΔE_{ONIOM}) with Δr_{LA} with respect to r_{LA}^0 , and the dependence of the oscillator strength ($f_{\text{model}}^{\text{high}}$, $f_{\text{model}}^{\text{low}}$, and f_{ONIOM}) on Δr_{LA} ,

**Figure 5.** $f_{\text{model}}^{\text{high}}$, $f_{\text{model}}^{\text{low}}$, and f_{ONIOM} dependence on Δr_{LA} (Å) for the substituted cyclopropenes.

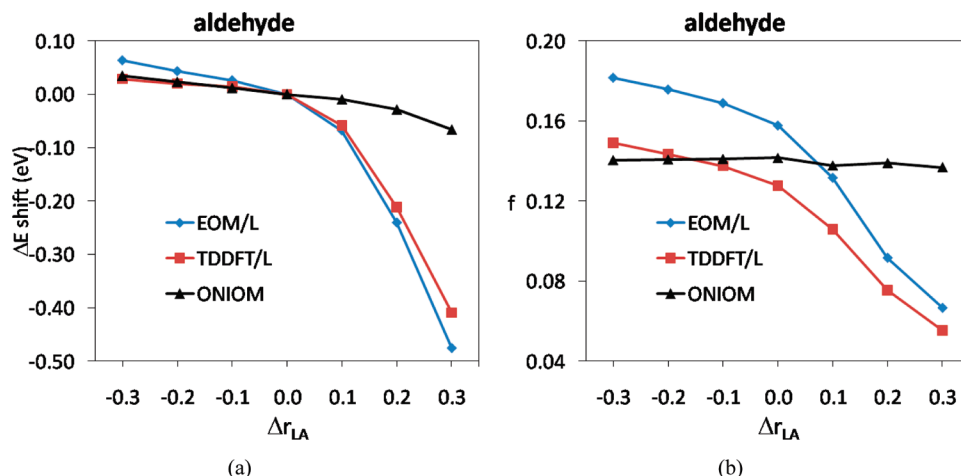


Figure 6. (a) $\Delta E_{\text{model}}^{\text{high}}$, $\Delta E_{\text{model}}^{\text{low}}$, and ΔE^{ONIOM} shift from r_{LA}^0 . (b) $f_{\text{model}}^{\text{high}}$, $f_{\text{model}}^{\text{low}}$, and f^{ONIOM} dependence on Δr_{LA} (Å) for the aldehyde.

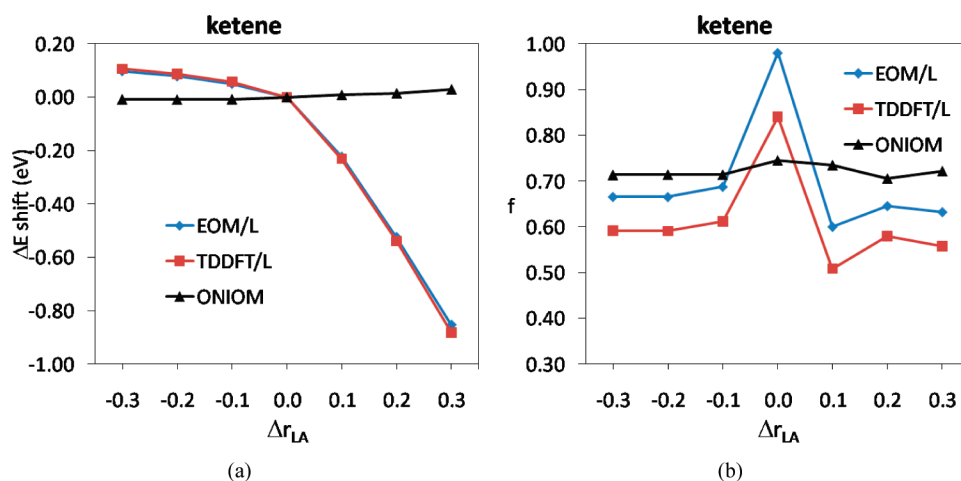


Figure 7. (a) $\Delta E_{\text{model}}^{\text{high}}$, $\Delta E_{\text{model}}^{\text{low}}$, and ΔE^{ONIOM} shift from r_{LA}^0 . (b) $f_{\text{model}}^{\text{high}}$, $f_{\text{model}}^{\text{low}}$, and f^{ONIOM} dependence on Δr_{LA} (Å) for the ketene. TDDFT in this case refers to the CAM-B3LYP functional.

shown in Figure 6. The precise value of r_{LA} ($r_{LA}^0 = 1.105$ Å; the other C–H bond is 1.107 Å) has a small effect on the ONIOM transition properties since the trend is the same for the *high* and *low* level methods, especially in the range ± 0.1 Å. Figure 7 reports the transition energy shift and the variation of the oscillator strength for the ketene. CAM-B3LYP is used in the *low* level, as this functional showed the best performance for this system. $f_{\text{model}}^{\text{high}}$ and $f_{\text{model}}^{\text{low}}$ obtained with r_{LA} distorted from r_{LA}^0 ($r_{LA}^0 = 1.102$ Å) decrease considerably because of the mixing with other excited states of the same symmetry and close in energy. The geometry at r_{LA}^0 is very close to the C_{2v} symmetry (the other C–H bond is 1.085 Å). The link atom slightly distorts the more symmetric geometry (the point group of the *model* system is C_s as in the *real* system) in order to represent the presence of the substituent group. However, further distortion produces the mixing of various states that is responsible for the underestimated values of $f_{\text{model}}^{\text{high}}$ and $f_{\text{model}}^{\text{low}}$ away from r_{LA}^0 . The values of $f_{\text{model}}^{\text{high}}$ and $f_{\text{model}}^{\text{low}}$ at the optimized C_{2v} geometry are 1.0038 and 0.8679, respectively, which are indeed very close to those reported in Table 6. Nonetheless, the dependence on r_{LA} is small in the ONIOM calculation.

5. Discussion and Conclusion

In this paper, we report calculations of oscillator strength with the ONIOM hybrid method. We consider four electronic excitations to valence states and compare the ONIOM results with the *target* calculation (EOM-CCSD on the entire system). We test various *low* levels of theory and check the dependence of the ONIOM results on the choice of the link atom bond length. We only define *model* systems that follow the ONIOM guidelines for partitioning.¹⁵

The conclusions in this paper closely follow our findings for the transition energy.^{16,17} We note that it is important to verify that the same states from the subcalculations are integrated. The *low* level method that gives the best balance between accuracy and computational savings is again TDDFT, although it is important to choose the right functional for a particular transition as shown by the ketene case. CIS and TDHF often provide poor results that make the improvement over $f_{\text{model}}^{\text{high}}$ not impressive, although an improvement over $f_{\text{real}}^{\text{low}}$ is obtained almost always. EOM-CCSD as a *low* level with a smaller basis set than the *target* usually provides the results closest to the *target*, but the $f_{\text{real}}^{\text{low}}$ (and $\Delta E_{\text{real}}^{\text{low}}$) calculation can be very demanding. Additionally, we find a case (the aldehyde) where the basis set for EOM-CCSD in

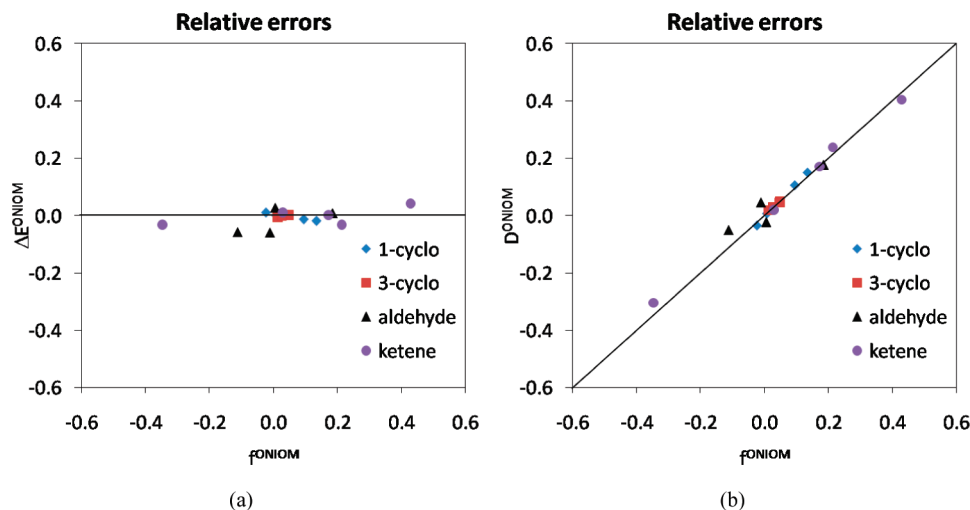


Figure 8. Relative errors of the transition energy (a) and dipole strength (b) compared to the relative errors of the oscillator strength. The ketene set includes the CAM-B3LYP results.

the *low* level calculation is not adequate and provides poor results. Therefore, the choice of the basis set is very important.

Relative timings are not reported in this paper, and we refer to ref 16 for a more detailed discussion. We only point out that the bottleneck calculation is $\Delta E_{\text{model}}^{\text{high}}$ for the systems presented here when a method such as TDDFT is used in the *low* level. Since a method like EOM-CCSD scales as $O(N^6)$, where N is the number of basis functions, it is evident that a hybrid method such as ONIOM can greatly reduce the computational effort by performing the expensive calculation only on the *model* system.

We confirmed that the definition of the link atom bond length (that follows the ground state formula) is appropriate also for this transition property. In fact, the dependence of f^{ONIAM} (as well as of ΔE^{ONIAM}) on the exact value of r_{LA} is small due either to a cancellation of errors between the *model* systems subcalculations or to a small dependence of the individual subcalculations.

Although the guidelines reported in refs 16 and 17 for the transition energy also hold for the oscillator strength, the latter is a much more sensitive quantity. This is shown in Figure 8, which reports the relative errors of ΔE^{ONIAM} and D^{ONIAM} as a function of the relative errors of f^{ONIAM} for all the *low* level methods. These graphs show that the relative errors for the oscillator strength are larger than those of the transition energy (the graphs also include the *low* level methods that do not perform very well as discussed in the previous section). Additionally, there is a direct relationship between the dipole and oscillator strengths errors. This is not surprising, as D^{ONIAM} is a quadratic quantity that depends on the independent extrapolation of the various components of the transition dipoles, eqs 4 and 5.

Our preliminary results therefore show that, although oscillator strengths are more sensitive than transition energies, they can be accurately computed with ONIOM provided that a sensible choice of the partitioning and of the *low* level method is made.

Supporting Information Available: Geometries of the aldehyde and the ketene and of their respective *model*

systems (for the geometries of the cyclopropenes, we refer to the supporting material of ref 16). This material is available free of charge via the Internet at <http://pubs.acs.org>.

References

- (1) Senn, H. M.; Thiel, W. *Angew. Chem., Int. Ed.* **2009**, *48*, 1198–1229.
- (2) Field, M. J.; Bash, P. A.; Karplus, M. *J. Comput. Chem.* **1990**, *11*, 700–733.
- (3) Singh, U. C.; Kollman, P. A. *J. Comput. Chem.* **1986**, *7*, 718–730.
- (4) Warshel, A.; Levitt, M. *J. Mol. Biol.* **1976**, *103*, 227–249.
- (5) Dapprich, S.; Komaromi, I.; Byun, K. S.; Morokuma, K.; Frisch, M. J. *THEOCHEM* **1999**, *461*, 1–21.
- (6) Svensson, M.; Humbel, S.; Froese, R. D. J.; Matsubara, T.; Sieber, S.; Morokuma, K. *J. Phys. Chem.* **1996**, *100*, 19357–19363.
- (7) Humbel, S.; Sieber, S.; Morokuma, K. *J. Chem. Phys.* **1996**, *105*, 1959–1967.
- (8) Vreven, T.; Morokuma, K. *J. Comput. Chem.* **2000**, *21*, 1419–1432.
- (9) Vreven, T.; Morokuma, K. In *Annual reports in computational chemistry*; Elsevier: Amsterdam, 2006; Vol 2, Chapter 3, pp 35–51.
- (10) Morokuma, K.; Musaev, D. G.; Vreven, T.; Basch, H.; Torrent, M.; Khoroshun, D. V. *IBM J. Res. Dev.* **2001**, *45*, 367–395.
- (11) Vreven, T.; Morokuma, K.; Farkas, O.; Schlegel, H. B.; Frisch, M. J. *J. Comput. Chem.* **2003**, *24*, 760–769.
- (12) Vreven, T.; Byun, K. S.; Komaromi, I.; Dapprich, S.; Montgomery, J. A.; Morokuma, K.; Frisch, M. J. *J. Chem. Theory Comput.* **2006**, *2*, 815–826.
- (13) Bearpark, M. J.; Ogliaro, F.; Vreven, T.; Boggio-Pasqua, M.; Frisch, M. J.; Larkin, S. M.; Morrison, M.; Robb, M. A. *J. Photochem. Photobiol., A* **2007**, *190*, 207–227.
- (14) Hall, K. F.; Vreven, T.; Frisch, M. J.; Bearpark, M. J. *J. Mol. Biol.* **2008**, *383*, 106–121.
- (15) Clemente, F. R.; Vreven, T.; Frisch, M. J. In *Quantum Biochemistry*; Wiley-VCH: Weinheim, Germany, 2010; Vol. 1, Chapter 2, pp 61–83.

- (16) Caricato, M.; Vreven, T.; Trucks, G. W.; Frisch, M. J.; Wiberg, K. B. *J. Chem. Phys.* **2009**, *131*, 134105.
- (17) Caricato, M.; Vreven, T.; Trucks, G. W.; Frisch, M. J. *J. Chem. Phys.* **2010**, *133*, 054104.
- (18) Sekino, H.; Bartlett, R. J. *Int. J. Quantum Chem., Quantum Chem. Symp.* **1984**, *18*, 255–265.
- (19) Geertsen, J.; Rittby, M.; Bartlett, R. J. *Chem. Phys. Lett.* **1989**, *164*, 57–62.
- (20) Stanton, J. F.; Bartlett, R. J. *J. Chem. Phys.* **1993**, *98*, 7029–7039.
- (21) Bartlett, R. J.; Musial, M. *Rev. Mod. Phys.* **2007**, *79*, 291–352.
- (22) Kallay, M.; Gauss, J. *J. Chem. Phys.* **2004**, *121*, 9257–9269.
- (23) Monkhorst, H. J. *Int. J. Quantum Chem.* **1977**, *Y11*, 421–432.
- (24) Koch, H.; Jorgensen, P. *J. Chem. Phys.* **1990**, *93*, 3333–3344.
- (25) Derat, E.; Bouquant, J.; Humbel, S. *THEOCHEM* **2003**, *632*, 61–69.
- (26) Becke, A. D. *J. Chem. Phys.* **1993**, *98*, 1372–1377.
- (27) Becke, A. D. *J. Chem. Phys.* **1993**, *98*, 5648–5652.
- (28) Stephens, P. J.; Devlin, F. J.; Ashvar, C. S.; Chabalowski, C. F.; Frisch, M. J. *Faraday Discuss.* **1994**, *99*, 103–119.
- (29) Yanai, T.; Tew, D. P.; Handy, N. C. *Chem. Phys. Lett.* **2004**, *393*, 51–57.
- (30) Peach, M. J. G.; Benfield, P.; Helgaker, T.; Tozer, D. J. *J. Chem. Phys.* **2008**, *128*, 044118.
- (31) Becke, A. D. *Phys. Rev. A* **1988**, *38*, 3098–3100.
- (32) Lee, C. T.; Yang, W. T.; Parr, R. G. *Phys. Rev. B* **1988**, *37*, 785–789.
- (33) Iikura, H.; Tsuneda, T.; Yanai, T.; Hirao, K. *J. Chem. Phys.* **2001**, *115*, 3540–3544.
- (34) Tawada, T.; Tsuneda, T.; Yanagisawa, S.; Yanai, T.; Hirao, K. *J. Chem. Phys.* **2004**, *120*, 8425–8433.
- (35) Frisch, M. J.; Trucks, G. W.; Schlegel, H. B.; Scuseria, G. E.; Robb, M. A.; Cheeseman, J. R.; Scalmani, G.; Barone, V.; Mennucci, B.; Petersson, G. A.; Nakatsuji, H.; Caricato, M.; Li, X.; Hratchian, H. P.; Izmaylov, A. F.; Bloino, J.; Zheng, G.; Sonnenberg, J. L.; Hada, M.; Ehara, M.; Toyota, K.; Fukuda, R.; Hasegawa, J.; Ishida, M.; Nakajima, T.; Honda, Y.; Kitao, O.; Nakai, H.; Vreven, T.; Montgomery, J. A., Jr.; Peralta, J. E.; Ogliaro, F.; Bearpark, M.; Heyd, J. J.; Brothers, E.; Kudin, K. N.; Staroverov, V. N.; Kobayashi, R.; Norm, J.; Raghavachari, K.; Rendell, A.; Burant, J. C.; Iyengar, S. S.; Tomasi, J.; Cossi, M.; Rega, N.; Millam, J. M.; Klene, M.; Knox, J. E.; Cross, J. B.; Bakken, V.; Adamo, C.; Jaramillo, J.; Gomperts, R.; Stratmann, R. E.; Yazyev, O.; Austin, A. J.; Cammi, R.; Pomelli, C.; Ochterski, J. W.; Martin, R. L.; Morokuma, K.; Zakrzewski, V. G.; Voth, G. A.; Salvador, P.; Dannenberg, J. J.; Dapprich, S.; Daniels, A. D.; Farkas, O.; Foresman, J. B.; Ortiz, J. V.; Cioslowski, J.; Fox, D. J. *Gaussian 09*; Gaussian, Inc.: Wallingford, CT, 2009.
- (36) Caricato, M.; Trucks, G. W.; Frisch, M. J.; Wiberg, K. B. *J. Chem. Theory Comput.* **2010**, *6*, 370–383.

CT1006289